

- (16) (a) Kato, Y.; Watanabe, M.; Sanui, K.; Ogata, N. *Solid State Ionics* **1990**, 40/41, 632. (b) Watanabe, M.; Nagano, S.; Sanui, K.; Ogata, N. *Solid State Ionics* **1988**, 28-30, 911. (c) Bruce, P.; Vincent, C. A. *J. Electroanal. Chem.* **1987**, 225, 1. (d) Evans, J.; Vincent, C. A.; Bruce, P. G. *Polymer* **1987**, 28, 2324.
- (17) Watanabe, M.; Longmire, L. L.; Murray, R. W. *J. Phys. Chem.* **1990**, 94, 2614.
- (18) Cohen, M. H.; Turnbull, D. *J. Chem. Phys.* **1959**, 31, 1164.
- (19) Adam, G.; Gibbs, J. H. *J. Chem. Phys.* **1965**, 43, 139.
- (20) Williams, M. L.; Landel, R. F.; Ferry, J. D. *J. Am. Chem. Soc.* **1955**, 77, 3701.
- (21) (a) Vogel, H. *Phys. Z.* **1921**, 22, 645. (b) Tamman, G.; Hesse, W. *Z. Anorg. Allg. Chem.* **1926**, 156, 245. (c) Fulcher, G. S. *J. Am. Ceram. Soc.* **1925**, 8, 339.
- (22) (a) Marcus, R. A. *J. Phys. Chem.* **1963**, 67, 853. (b) Marcus, R. A. *Annu. Rev. Phys. Chem.* **1964**, 15, 155. (c) Marcus, R. A. *J. Chem. Phys.* **1965**, 43, 679. (d) Marcus, R. A.; Sutin, N. *Biochim. Biophys. Acta* **1985**, 811, 265.
- (23) Wooster, T. T.; Longmire, M. L.; Zhang, H.; Watanabe, M.; Murray, R. W. *Anal. Chem.*, in press.
- (24) Long, R. E.; Sparks, R. A.; Trueblood, K. N. *Acta Crystallogr.* **1965**, 18, 932.
- (25) (a) Chidsey, C. E. D. *Science* **1991**, 251, 919. (b) Brunschwig, B. S.; Ehrenson, S.; Sutin, N. *J. Am. Chem. Soc.* **1984**, 22, 6858. (c) Axup, A. W.; Albin, M.; Mayo, S.; Crutchley, R. J.; Gray, H. J. *Am. Chem. Soc.* **1988**, 110, 435. (d) McLendon, G. *Acc. Chem. Res.* **1988**, 21, 160.
- (26) Fritsch-Faules, I.; Faulkner, L. R. *J. Electroanal. Chem.* **1989**, 263, 237.
- (27) (a) Murray, R. W. *Annu. Rev. Mater. Sci.* **1984**, 14, 145. (b) Chidsey, C. E. D.; Murray, R. W. *J. Phys. Chem.* **1986**, 90, 1479. (c) Murray, R. W., Ed. *Molecular Design of Electrode Surfaces*; Wiley: New York, 1992.
- (28) (a) Nielson, R. M.; McManis, G. E.; Golovin, M. N.; Weaver, M. J. *J. Phys. Chem.* **1988**, 92, 3441. (b) McManis, G. E.; Weaver, M. J. *Chem. Phys. Lett.* **1988**, 145, 55. (c) Zhang, X.; Leddy, J.; Bard, A. J. *J. Am. Chem. Soc.* **1985**, 107, 3719. (d) Zhang, X.; Yang, H.; Bard, A. J. *J. Am. Chem. Soc.* **1987**, 109, 1916. (e) Weaver, M. J.; Gennett, T. *Chem. Phys. Lett.* **1985**, 113, 213. (f) Gennett, T.; Milner, D. F.; Weaver, M. J. *J. Phys. Chem.* **1985**, 89, 2787. (g) McManis, G. E.; Golovin, M. N.; Weaver, M. J. *J. Phys. Chem.* **1986**, 90, 6563. (h) Nielson, R. M.; Weaver, M. J. *J. Electroanal. Chem.* **1989**, 260, 15. (i) Kapturkiewicz, A.; Behr, B. *J. Electroanal. Chem.* **1984**, 179, 187. (j) Kapturkiewicz, A.; Opallo, M. *J. Electroanal. Chem.* **1985**, 185, 15. (k) Opallo, M. *J. Chem. Soc., Faraday Trans. 1* **1987**, 83, 161.
- (29) (a) Nielson, R. M.; McManis, G. E.; Safford, L. K.; Weaver, M. J. *J. Phys. Chem.* **1989**, 93, 2152. (b) Weaver, M. J.; Phelps, D. K.; Nielson, R. M.; Golovin, M. N.; McManis, G. E. *J. Phys. Chem.* **1990**, 94, 2949.

Aperiodicity and Deterministic Chaos in the Belousov-Zhabotinsky Reaction

R. Blittersdorf, A. F. Münster, and F. W. Schneider*

Institute of Physical Chemistry, University of Würzburg, Marcusstrasse 9-11, D-8700 Würzburg, Germany
(Received: February 12, 1992)

Deterministic chaos in the Belousov-Zhabotinsky reaction is well-known to occur at low flow rates.¹⁻⁶ However, the source of aperiodicity in the high flow rate region has remained a controversial issue. We reproduced the aperiodicity found by Hudson^{7,8} and, more recently, by Noszticzius et al.⁹ under practically identical experimental conditions. We interpret the observed aperiodicity at high flow rates as nonchaotic on the basis of the 1-D maps and Renyi dimensions (calculated with the nearest neighbor method¹¹⁻¹³ from single value decomposition reconstructed¹⁰ attractors), including the Hausdorff dimension. The observed aperiodicity at high flow rates is most probably a noisy time series of the 1¹2 state and the adjoining Farey ordered states.

Introduction

The existence of deterministic chaos in a continuous flow stirred tank reactor (CSTR) at low flow rates in the Belousov-Zhabotinsky (BZ) reaction was clearly demonstrated by Swinney and co-workers¹⁻⁴ and later verified by us.^{5,6} Aperiodic time series can also be observed at high flow rates as first shown by Hudson et al.^{7,8} and later by Noszticzius et al.⁹ who interpreted these high flow rate experiments in terms of deterministic chaos.

We reproduced the high flow rate Hudson and Noszticzius experiments under identical experimental conditions of temperature, concentrations, Pt-redox and Br⁻-selective electrodes and a reactor of comparable volume (10.8 mL). We obtained practically identical experimental results as those of the latter authors. On the basis of one-dimensional maps and the dimensionality of the attractors (e.g. Hausdorff, information and correlation dimensions) we interpret the high flow rate aperiodicity to arise from statistical fluctuations between Farey ordered periodic states rather than from deterministic chaos.

Other measures such as Fourier spectra, Poincaré sections, and maximum Lyapounov exponents were not found to be suitable in this case to critically distinguish between deterministic chaos and aperiodic motion which is generated by statistical switching between periodic states. This confirms our earlier work at high flow rates on the same subject^{5,6} in which optical detection of [Ce⁴⁺] in a small compact reactor (1.70 mL) also showed the existence of noise-related aperiodicities. A juxtaposition of the aperiodicities at low and high flow rates shows the generic difference between these two types of aperiodicities.

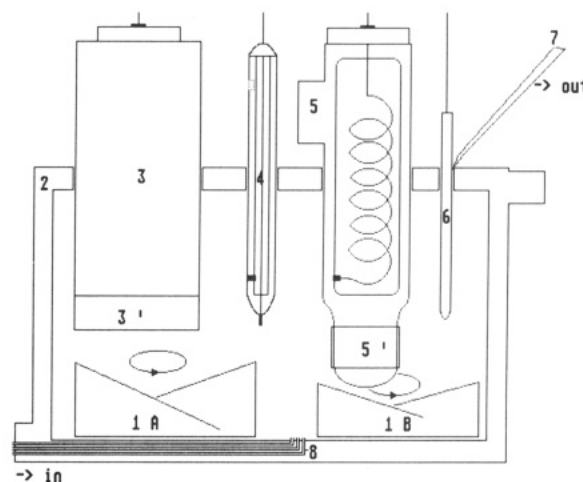


Figure 1. Schematic drawing of the reactor: 1 A, 1 B, magnetic stirrers; 2, thermostated reactor; 3, Br⁻ selective electrode with membrane (3'); 4, Pt-redox electrode; 5, reference electrode with membrane (5'); 6, thermocouple; 7, outlet under aspirator vacuum; 8, three inlets for the reactant solutions.

Experimental Section

Materials. Malonic acid (Sigma) was recrystallized from acetone in a similar method to that described by Noszticzius et al.⁹ KBrO₃ (Merck) with bromide concentration less than 0.02%, CeSO₄ (Fluka, 99.99%) and H₂SO₄ (Merck, 97%) were used without further purification.

* Author to whom correspondence should be addressed.

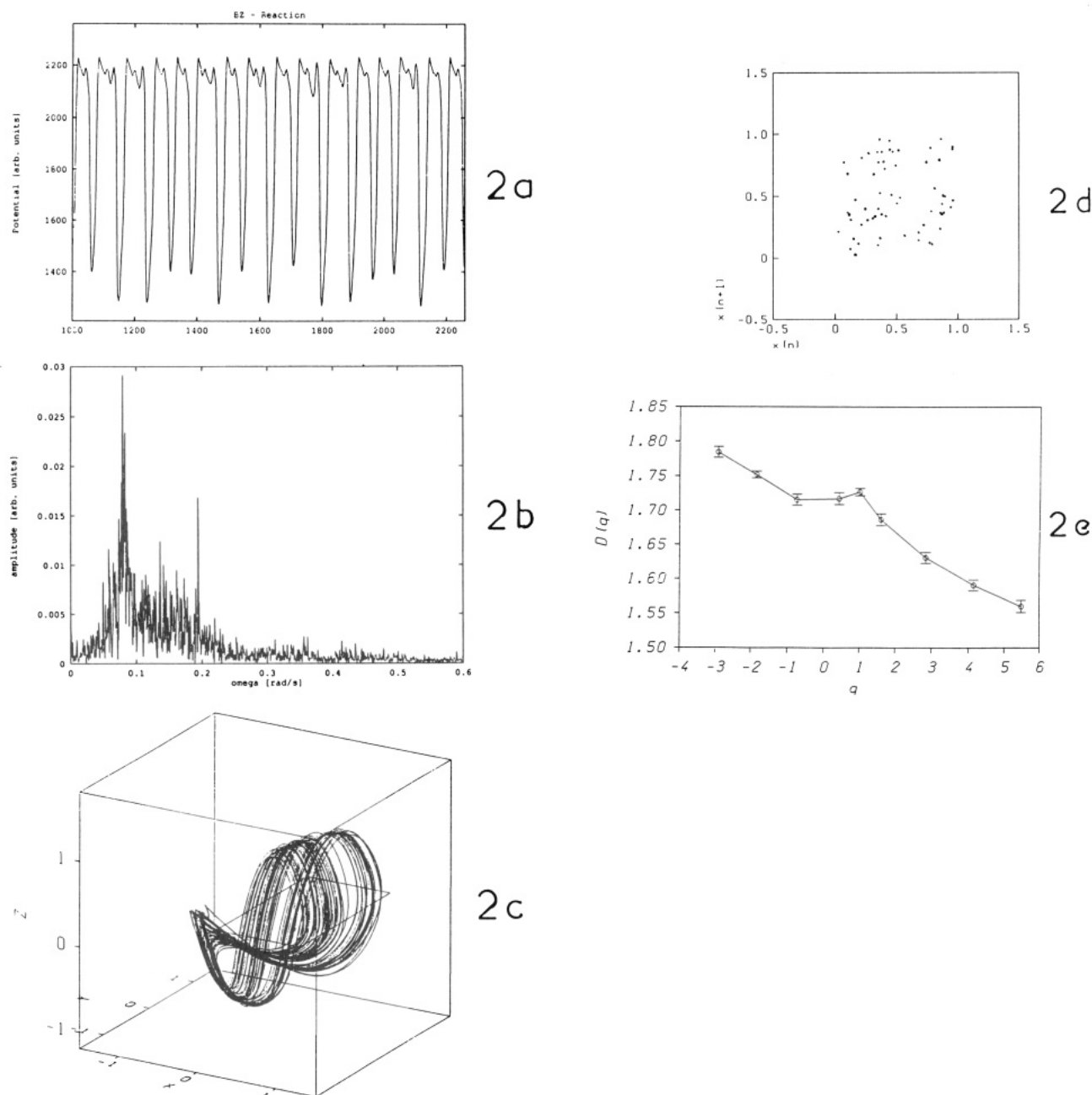


Figure 2. Time series, Fourier spectrum, attractor, 1-D map, and spectrum of dimensions of a high flow rate ($k_f = 0.209 \text{ min}^{-1}$) experiment, measured with a bromide ion sensitive electrode: (a) part of a longer time series (6000 s); (b) Fourier spectrum; (c) attractor, calculated with the SVD method;¹⁰ (d) 1-D map; (e) spectrum of dimensions, calculated with the NNA method,¹¹⁻¹³ where the maximum order of nearest neighbors was $k = 800$: $q \rightarrow 0$, Hausdorff dimension ($D_0 = \text{geometrical dimension}$); $q \rightarrow 1$, $D_1 = \text{information dimension}$; $q \rightarrow 2$, $D_2 = \text{correlation dimension}$.

Reactor and Stirring. A schematic drawing of the reactor is shown in Figure 1. Its volume is 10.8 cm^3 as compared with the 10.7-cm^3 volume of the Noszticzius reactor.⁹ The Plexiglas reactor has a cuboid shape. Efficient stirring was provided by two unsymmetric magnetic stirrers driven by separate small motors located beneath the reactor. Varying the stirring rate between 1000 and 1500 rpm for both stirrers had no effect on the results. For all of the experiments shown in this work the stirring rate was maintained constant at 1200 rpm.

Concentrations. The reactor concentrations were chosen to be identical with those of the Hudson and Noszticzius experiments:⁷⁻⁹ [malonic acid] = 0.30 M, $[\text{BrO}_3^-]$ = 0.14 M, $[\text{Ce}^{3+}]$ = 1.0×10^{-3} M, $[\text{H}_2\text{SO}_4]$ = 0.20 M.

All solutions were degassed before each measurement to reduce the formation of bubbles of CO_2 produced in the chemical reaction. A small drift in the flow rate (up to 1%) was probably caused by formation of CO_2 bubbles.

Three feedlines containing malonic acid and CeSO_4 , KBrO_3 , and H_2SO_4 were used.

Electrodes. A bromide ion selective electrode (Ingold 152113000) with a Ag_2S pellet membrane and a reference electrode (Ingold 373-90-WTE-ISE-S7) with a KNO_3 electrolytic bridge were employed. In addition, a platinum redox electrode (Ingold Pt 4800-M5) was used to measure the redox potential, which depends primarily on the $\text{Ce}^{3+}/\text{Ce}^{4+}$ concentration. The Br^- selective electrode was calibrated with solutions of known Br^- concentrations. During the measurement its potential varied between 170–220 mV, corresponding to Br^- concentrations in the range of 8×10^{-6} to 3×10^{-5} M.

Pumps. A self-designed high-precision syringe pump driven by a stepping motor was employed to control the flow rate of reactants into the CSTR. Each step of the motor moves the syringe piston 100 nm, which corresponds to $0.22 \mu\text{L}$ of flow volume per pulse. The period between motor steps is electronically controlled with high precision. Typical stepping frequencies for our measurements of the BZ reaction were in the range of 10–300 Hz. Therefore, the liquid flow into the reactor is practically constant. Gas-tight syringes (Fortuna) deliver the above solutions

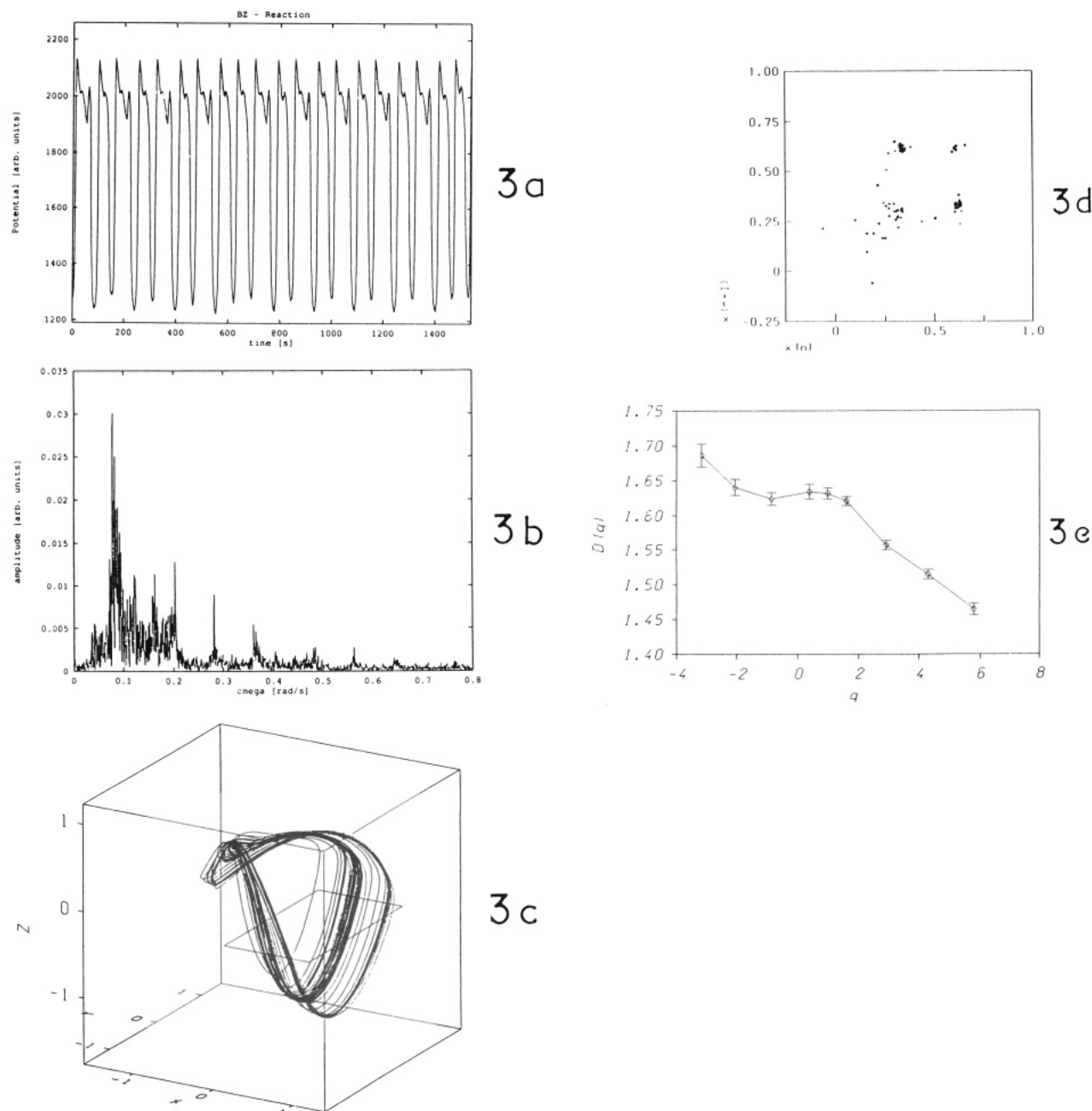


Figure 3. Time series, Fourier spectrum, attractor, 1-D map, and spectrum of dimensions of a high flow rate ($k_f = 0.209 \text{ min}^{-1}$) experiment, measured with a platinum redox electrode: (a) part of a longer time series (6000 s); (b) Fourier spectrum; (c) attractor, calculated with the SVD method;¹⁰ (d) 1-D map; (e) spectrum of dimensions, calculated with the NNA method,^{11–13} where $k = 800$.

into the CSTR at constant flow rates.

Temperature. The syringes containing the input chemicals, the tubing and the reactor were thermostated (Figure 1). The temperature inside the reactor was $25.0 \pm 0.1^\circ \text{C}$ for all experiments as indicated by a thermocouple in the reactor.

Results and Analysis

Reproduction of the Hudson and Noszticzius Experiments.^{7–9}

Figures 2 and 3 show experimental time series, Fourier spectra, attractors, 1-D maps, and dimensions D_q in the high flow rate region between two Farey ordered states 1^1 ($k_f = 0.187 \text{ min}^{-1}$) and 1^2 ($k_f = 0.216 \text{ min}^{-1}$). The time series are very similar to those of the Hudson and Noszticzius experiments. In this work the attractors were reconstructed by singular value decomposition (SVD).¹⁰ The SVD method was found in model calculations (Brusselator¹⁴ and extended Oregonator²³ with superimposed noise) to be more reliable than the Takens method in the case of inhomogeneous noisy attractors. The one-dimensional (1-D) maps were constructed from the Poincaré sections (not shown). For

the calculation of the dimensionalities we implemented the nearest neighbor analysis (NNA)^{11–13} which leads to a spectrum of generalized Renyi dimensions. These are defined as follows: Consider a sequence of points $x(t=0, x(t=\tau), \dots, x(t=N\tau)$ which lies on an orbit of an attractor. If the phase space is partitioned into cells of size l , the probability P_i of a point being in cell i is $P_i = \lim_{N \rightarrow \infty} N_i/N$. The Renyi information of order q , which is related to the q th power of P_i , is defined as^{12,13,15}

$$S_l^q = \frac{1}{1-q} \ln \sum_{i=1}^N P_i^q$$

The generalized dimensions D_q are related to the Renyi information as follows

$$D_q = \lim_{l \rightarrow 0} \frac{S_l^q}{\ln(1/l)}$$

The width of the spectrum of the D_q values reflects the nonuniformity of an attractor: Negative values of q correspond to the

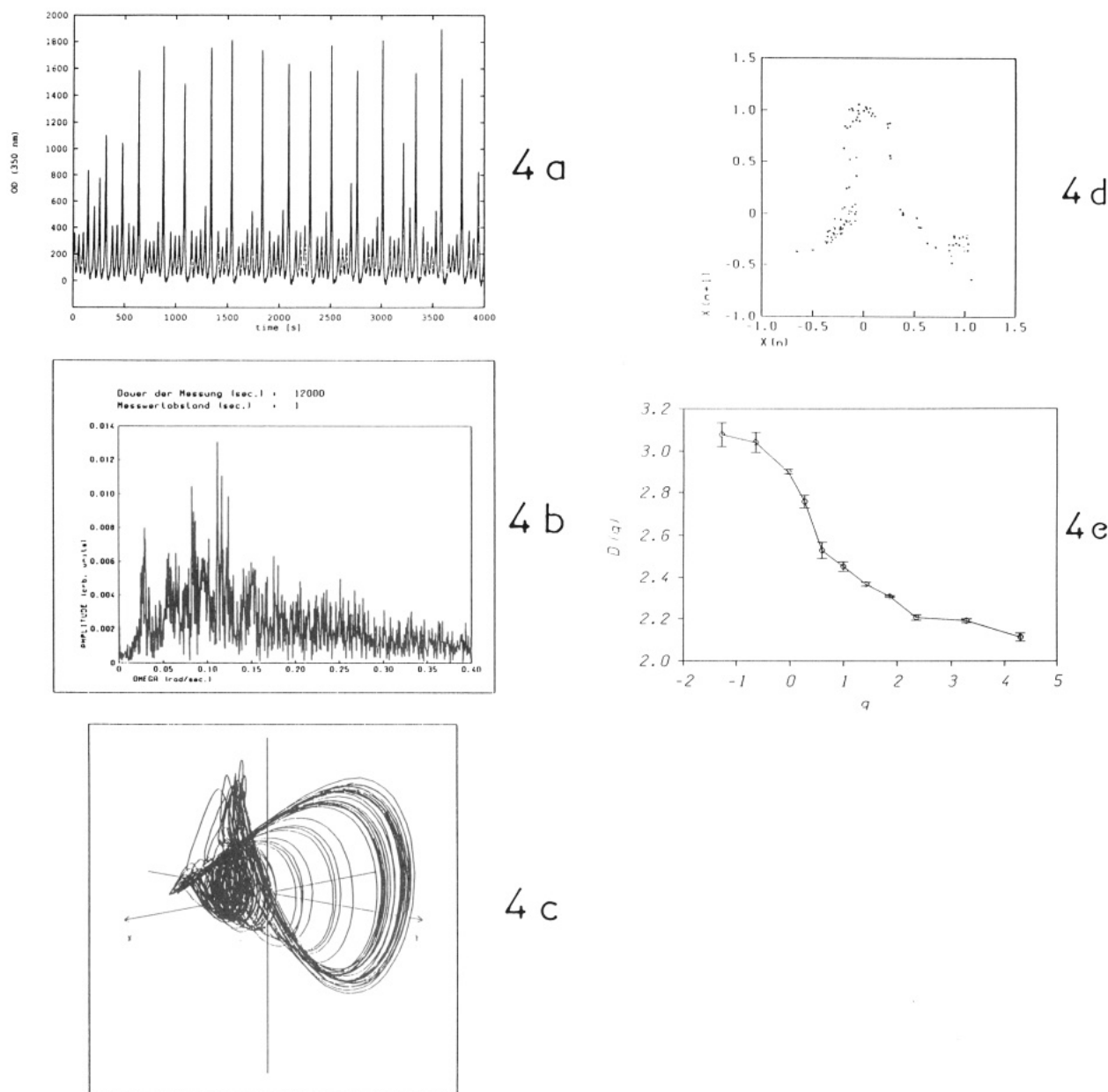


Figure 4. Time series, Fourier spectrum, attractor, 1-D map, and spectrum of dimensions of a low flow rate ($k_f = 1.6 \times 10^{-2} \text{ min}^{-1}$) experiment, measured by UV detection of the aqueous $[\text{Ce}^{4+}]$ at $\lambda = 350 \text{ nm}$: (a) part of a longer time series (6000 s); (b) Fourier spectrum; (c) attractor, calculated with the SVD method;¹⁰ (d) 1-D map; (e) spectrum of dimensions, calculated with the NNA method,¹¹⁻¹³ where $k = 800$.

rarely visited regions of the attractor whereas positive q values emphasize the frequently visited regions where the density of points is high. It can be shown that the Hausdorff dimension corresponds to the limit $q \rightarrow 0$, the information dimension to $q \rightarrow 1$ and the correlation dimension to $q \rightarrow 2$.¹⁶ In the NNA calculation the maximum order of the nearest neighbors was varied between 400 and 1600 without significant effects on the results.

For an internal check we independently calculated the Hausdorff dimension by the box counting algorithm^{17,18} ($D_0 = 1.70$; calculated from 6000 data points, maximum imbedding dimension of 10, weighted by the singular values), the information dimension by the box and sphere counting^{15,19} methods ($D_1 = 1.65$), and also the correlation dimension by the sphere counting method ($D_2 = 1.60$; parameters for the calculation as above; 500 reference points) for the aperiodicity at the high flow rate of $k_f = 0.209 \text{ min}^{-1}$.

For comparison, we also show our measurements of deterministic chaos at low flow rates carried out in a small, compact reactor ($V = 1.70 \text{ mL}$) with optical detection of $[\text{Ce}^{4+}]$ (Figure 4a) together with the Fourier spectrum (Figure 4b), SVD attractor (Figure 4c), 1-D map (Figure 4d), and the calculated D_q spectrum (Figure 4e).

Discussion

In earlier investigations at high flow rates⁵ we demonstrated the presence of multi peaked oscillation patterns whose sequence is determined by the Farey arithmetic²⁰ as already observed by Maselko and Swinney in the Mn-catalyzed BZ reaction.²¹ When L^S represents the Farey pattern where L and S correspond to large (L) and small (S) amplitude peaks, we observed the following patterns 2^1 , $2^1 2^2$, 2^2 , $2^2 2^3$, and 2^3 in the k_f range from 0.154 to 0.205 min^{-1} . As shown by Lamba and Hudson²² it is possible to switch from the 1^1 to the 2^2 pattern by a single flow perturbation (i.e. stopping the pump for $\sim 10 \text{ s}$) and from the 2^2 to the 1^1 pattern by a single perturbation imposed on the stirring rate (i.e. stopping the stirrer for $\sim 10 \text{ s}$). Thus it may be shown²³ that the sequence 1^1 , $1^1 1^2$, and 1^2 may replace the above sequence 2^2 , $2^2 2^3$, and 2^3 . In agreement with Noszticzus et al.,⁹ our high flow rate results were not sensitive toward trace impurities (Fe^{3+} , formaldehyde) or stirring rate (1000–1500 rpm). On the other hand we could resolve the fine structure 1^1 , $1^1 1^2$, 1^2 only in a well-stirred, compact reactor ($V = 1.70 \text{ mL}$) with optical detection of Ce(IV) ²³ (Figure 5). We estimate the k_f width of the $1^1 1^2$ pattern to be

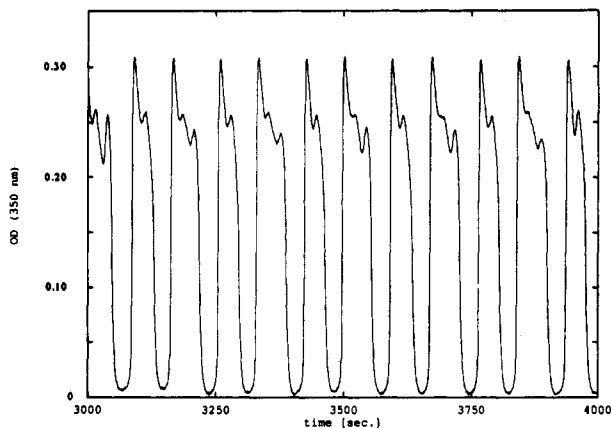


Figure 5. Time series, showing the $1^1 1^2$ Farey pattern at a high flow rate ($k_f = 0.204 \text{ min}^{-1}$) in a compact reactor ($V = 1.70 \text{ mL}$).

maximally 1%, whereas the k_f width of the 1^1 and 1^2 pattern is larger (i.e. $\sim 3\text{--}4\%$ and $2\text{--}3\%$, respectively). Thus in reactors of large volumes ($\geq 10 \text{ mL}$) as in the experiments by Hudson,^{7,8} Noszticzius,⁹ and in this work (Figures 2 and 3), the $1^1 1^2$ Farey pattern is not resolved. Instead of the Farey pattern $1^1 1^2$, an aperiodic time series is observed which has been termed chaotic by Hudson^{7,8} and Noszticzius et al.,⁹ whereas the 1^1 and 1^2 patterns remain. Thus we have observed the same sequence of states in our larger reactor, namely 1^1 , aperiodic state, and 1^2 , as Hudson and Noszticzius et al., although there are some differences in the absolute values of the flow rates. We did not find any significant differences between the respective k_f values in our large and small reactor (Figures 2, 3, and 5). Our analysis of this aperiodic state demonstrates that it is not chaotic as based on the 1-D maps and the dimensionalities of the attractors:

The 1-D maps (Figures 2d and 3d) for the Br^- electrode and the platinum electrode, respectively, show a cloud of points typical for an aperiodic time series as generated by noise. The 1-D map shown by Hudson and Mankin⁸ (their Figure 5) is similar to 1-D maps obtained for the nonchaotic extended Oregonator with noise superimposed on the variables or the flow rate.²³ In contrast, the low flow rate chaos (Figure 4d) shows the contours of a distinct curve with an extremum typical of deterministic chaos.

Our NNA analysis shows the values of all calculated dimensionalities to be less than 2.0 for the high flow rate experiments (Figures 2e and 3e). The NNA results are in good agreement with independent calculations of the Hausdorff dimension, the information dimension, and the correlation dimension. In contrast, the chaotic time series at low flow rates shows a D_q spectrum between 3.1 and 2.1 for $q = -1.5$ and $q = 4$, respectively (Figure 4e). For low flow rates, all D_q values were found to be greater than 2.0, as is characteristic of deterministic chaos. Independent calculations of D_0 ($=2.55$), D_1 ($=2.42$), and D_2 ($=2.23$) were also found to be above 2.0, confirming the notion that deterministic chaos exists at low flow rates only.

We would like to emphasize that the Fourier spectra (Figures 2b, 3b, and 4b) and the attractors (Figures 2c, 3c, and 4c) do not permit distinction between noise-generated aperiodicity and chaos.

The same is true for the maximum Lyapounov exponents which are found to be always positive for deterministic chaos as well as random switching between neighboring limit cycles.^{5,25,26} In the distinction between noise and deterministic chaos, the Hausdorff dimension D_0 is particularly useful and important, since it represents the geometric dimension of the attractor. Thus, at high flow rates D_0 is 1.70 indicating a noisy aperiodicity, whereas at low flow rates D_0 is above 2.0, namely 2.55, indicating the presence of deterministic chaos. Noszticzius et al. do not show any Fourier spectra, 1-D maps, or dimensional analysis in their paper.⁹ They mainly base their argumentation for deterministic chaos at high flow rates on their simulations of a model^{9,24} and on the reproduction of the Hudson experiments, whereas the conclusions of this work are based on the experimental 1-D maps and the experimental D_q spectra including the Hausdorff dimension. Thus, according to the latter measures there seems to be no experimental evidence for deterministic chaos at high flow rates in the BZ reaction.

Acknowledgment. This work was supported by the Stiftung Volkswagenwerk and the Fonds der Chemischen Industrie. We thank T. M. Kruehl for the implementation of computer programs for the dimensional analysis. We thank Dr. Z. Noszticzius for a preprint of ref 9.

Registry No. BrO_3^- , 15541-45-4; Ce, 7440-45-1; malonic acid, 141-82-2.

References and Notes

- Turner, J. S.; Roux, J. C.; McCormick, W. D.; Swinney, H. L. *Phys. Lett.* **1981**, *85A*, 9.
- Simoyl, R. H.; Wolf, A.; Swinney, H. L. *Phys. Rev. Lett.* **1982**, *49*, 245.
- Coffman, K. G.; McCormick, W. D.; Noszticzius, Z.; Simoyl, R. H.; Swinney, H. L. *J. Chem. Phys.* **1987**, *86*, 119.
- Noszticzius, Z.; McCormick, W. D.; Swinney, H. L. *J. Phys. Chem.* **1987**, *91*, 5129.
- Münster, A. F.; Schneider, F. W. *J. Phys. Chem.* **1991**, *95*, 2130.
- Schneider, F. W.; Münster, A. F. In *Dissipative Structures in Transport Processes and Combustion*; Springer Series in Synergetics; Springer-Verlag: Berlin, 1990; p 169.
- Hudson, J. L.; Hart, M.; Marinko, D. *J. Chem. Phys.* **1979**, *71*, 1601.
- Hudson, J. L.; Mankin, J. C. *J. Chem. Phys.* **1981**, *74*, 6171.
- Györgyi, L.; Field, R. J.; Noszticzius, Z.; McCormick, W. D.; Swinney, H. L. *J. Phys. Chem.* **1992**, *96*, 1228.
- Broomhead, D. S.; King, G. P. *Physica* **1986**, *20D*, 217.
- Rényi, A. *Probability Theory*; North-Holland: Amsterdam, 1970.
- Van de Water, W.; Schram, P. *Phys. Rev. Lett.* **1988**, *37*, 3118.
- Badii, R.; Politi, A. *Phys. Rev. Lett.* **1984**, *52*, 1661.
- Freund, A. Ph.D. Thesis, 1988.
- Grassberger, P.; Procaccia, I. *Physica* **1983**, *9D*, 189.
- Marek, M. *Chaotic Behavior of Deterministic Dissipative Systems*; Academia: Praha, 1991; p 45.
- Reference 16, p 117.
- McGuinness, M. J. *Physica D* **1985**, *16*, 265.
- Grassberger, P.; Procaccia, I. *Phys. Rev. Lett.* **1983**, *50*, 346.
- Farey, J. *Philos. Mag. J.* **1816**, *47*, 385.
- Maselko, J.; Swinney, H. L. *J. Chem. Phys.* **1986**, *85*, 6430.
- Lamba, P.; Hudson, J. L. *Chem. Eng. Commun.* **1985**, *32*, 369.
- Münster, A. F. Ph.D. Thesis, 1992.
- Györgyi, L.; Field, R. J. *J. Phys. Chem.* **1992**, *96*, 1220.
- Kruehl, T. M.; Freund, A.; Schneider, F. W. *J. Chem. Phys.* **1990**, *93*, 416.
- Herzel, H.; Ebeling, W. *Z. Naturforsch.* **1987**, *42A*, 136.